Compensation of timing jitter-induced distortion of sampled waveforms

Jan Verspecht
HP-NMDG / VUB-ELEC
Pleinlaan 2
1050 Brussels (Belgium)

Compensation of timing jitter-induced distortion of sampled waveforms

Jan Verspecht

Abstract

The presence of timing jitter between the trigger signal and the sampling strobe in an equivalent-time sampling oscilloscope causes distortion of the recorded waveform. Two methods exist to estimate the waveform from the jittered measurements. One method, called the "median" method, is based on the calculation of the point-by-point median of a large set of waveform measurements. In this article it is shown that this method is asymptotically biased if noise is present and if the waveform is nonmonotonic. Another method, called the "pdf deconvolution" method, is based on an estimation of the jitter probability density function and on a technique to deconvolve this density function from the average of all recorded waveforms. To estimate the jitter probability density function, it is assumed that the waveform has a part which can very well be approximated by a ramp during a time span which is smaller than the standard deviation. In this article it is shown that a significant asymptotic bias is introduced by the method when this assumption is violated. A novel approach is proposed, based on a parametric model of the jitter probability density function, which results in an asymptotic unbiased estimate of the jitter probability density function. The method is experimentally verified, and it is explained why this method is especially useful when one is interested in the Fourier spectrum of the recorded waveform.

Keywords

timing jitter, sampling oscilloscope, distortion, Fourier transform, convolution, parametric model, probability density function, characteristic function

1. Introduction

"Time jitter" can cause significant systematic errors when waveforms are recorded with equivalent-time sampling oscilloscopes. The presence of time jitter means that every sample taken by the oscilloscope can only be situated on the time axis with a certain probability. This timing jitter causes systematic errors in the estimate of the measured waveform which are very hard to compensate because the jitter is a stochastic process very much dependent on the oscilloscope as well as the quality of the trigger signal. This means that the effect of the jitter will be different whenever we use another oscilloscope or another trigger signal! In the literature two methods are encountered that deal with waveform distortions due to time jitter: the so-called "median" method [1] and the so-called "pdf deconvolution" method [2]. The "median" method is based on the calculation of the point-by-point median of a large set of waveform measurements. In their article [1] Souders, Flach, Hagwood and Yang show that the estimate of the true

waveform will be asymptotically biased when this waveform is nonmonotonic. In this article it is explained that the presence of additive noise also introduces a bias. These two sources of bias make the method useless if one wants an accurate estimation of a pulse waveform. The "pdf deconvolution" method is based on an estimation of the jitter probability density function (pdf) and on a technique to deconvolve this density function from the average of all recorded waveforms. The accuracy of this method is very much dependent on the quality of the estimate of the jitter probability density function. In his article [2] Gans uses a portion of the waveform that can be approximated by an ideal ramp and a measurement of the apparent additive noise pdf at one time instant to estimate the jitter pdf. Although useful in many practical cases, an asymptotic bias is present when no part of the waveform can be approximated very well by a ramp, as is the case for pulses when the time jitter standard deviation becomes too large relative to the pulse transition duration. In this article a novel method is proposed which results in an asymptotic unbiased estimate of the jitter pdf. The method extends the use of the "pdf deconvolution" method to cases where the "ideal ramp approximation" approach can no longer be used. The method is based on the identification of the parameters of a parametric model of the jitter probability density function. For the purpose of the parameter identification, an error function is minimized which is a function of the parameters, the mean of the measured waveforms and the mean of the square of the measured waveforms.

In this paper, the method is derived mathematically, and it is shown what algorithm may be used to identify the parameters of a parametric model for the jitter pdf. It is explained how the effect of additive noise is effectively removed. A comparison is made between the "median" method and the novel method, based upon simulated data. Next the problems arising when applying the method of Gans [2] to estimate the jitter pdf are explained by illustrating the asymptotic bias of the method. Finally, the new method is applied to experimental data, illustrating its performance when the jitter standard deviation is large.

2. Mathematical equations of the extended "pdf deconvolution" method

For simplicity it is assumed that the sample rate with which the waveform is digitized is high enough to avoid aliasing and that care has been taken to avoid leakage problems. With these assumptions all continuous equations derived can easily be used for a digitized equivalent.

We assume that the jitter process can be characterized by a single pdf for all sampling instants. This pdf and the undistorted waveform are the two unknowns. The two things that will be measured are the point-by-point average of all measured waveforms, and the point-by-point average of all measured waveforms squared (first squaring and then averaging). In fact, these two functions will be equivalent to using the mean and the variance of a set of recorded waveforms. At this point it should be clear to the reader that this variance is not a constant at all sampling instants when time jitter is present, but will be larger at those sampling instants where the slope of the waveform is larger.

Notations:

$x(t)$: undistorted true signal

$a(t)$: expectation of the measured signal (infinite number of averages)

$s(t)$: expectation of the square of the measured signal (infinite number of averages)

$p(t)$: time jitter probability density function

$X(\omega)$, $A(\omega)$, $S(\omega)$, $P(\omega)$: Fourier transforms of x, a, s and p

In practice it will be possible to estimate a(t) and s(t) in an asymptotic unbiased manner by recording many waveforms and by calculating the mean (a(t)) and the mean of the waveforms squared (s(t)). It is possible to construct a set of equations describing the dependency of A and S on X and P.

In (1) the expectation of the measured waveform is calculated:

$$a(t) = \int_{-\infty}^{\infty} x(t-\tau)p(\tau)d\tau \quad . \tag{1}$$

In this equation τ is the stochastic variable indicating the amount of jitter at a certain moment of time, which shows up as a delay applied to the original signal. Equation (1) shows us that a(t) (this is the waveform we measure after having applied an infinite number of averages) is actually the convolution of the true signal x(t) and the probability density function of the jitter noise p(t). In the frequency domain this equation has the following form:

$$A(\omega) = X(\omega)P(\omega) \quad . \tag{2}$$

The measured, averaged waveform spectrum equals the original signal spectrum $X(\omega)$ multiplied by the characteristic function $P(\omega)$ of the jitter noise. $P(\omega)$ is the Fourier transform of the jitter noise probability density function. The idea developed in the article by Gans [2] is to measure $p(\tau)$ and to deconvolve it from the measured signal a(t). The main problem of course is how to measure $p(\tau)$. Instead of trying to measure $p(\tau)$ in a direct manner, which in some cases is hard to accomplish, a second equation independent of (2) can be derived. Equation (3) gives the relationship between s(t) and the two unknowns x(t) and $p(\tau)$. Similar to the case of a(t) in (1), s(t) is the convolution of the square of x(t) and the pdf of the jitter noise $p(\tau)$. That is,

$$s(t) = \int_{-\infty}^{\infty} x^2(t-\tau)p(\tau)d\tau \quad . \tag{3}$$

In the frequency domain this equation becomes

$$S(\omega) = (X*X)(\omega)P(\omega) \tag{4}$$

and (4) shows that $S(\omega)$ equals the product of $P(\omega)$ and the (frequency domain) convolution of $X(\omega)$ with itself.

The final set of equations relating A and S, the measured-waveform spectra, and the unknowns X and P are

$$A(\omega) = X(\omega)P(\omega)$$
$$S(\omega) = (X*X)(\omega)P(\omega) \quad .$$

According to the knowledge of the author, no algorithm is available in the literature to solve such a set of equations for a general P and X. When a parametric model for $P(\omega)$ is proposed, however, it will become possible to estimate the parameters with good accuracy by minimizing an error function based upon (2) and (4). Before going into this, the following section will cover the effects of additive noise.

3. Effects of additive noise

In experimental data additive noise will always be present. This noise, assumed here to be white, will cause minor problems for the algorithm. This can be shown as follows.

In practice a(t) and s(t) will be estimated by taking the average of many realizations of the measured signal and the square of the measured signal. One realization of the measured signal can be described as $x_m(t) = x(t-\tau) + n(t)$. In this equation τ is a realization of the stochastic jitter variable (τ has a different value for each t), and n stands for a realization of the stochastic zero-mean additive noise variable. Now the relation between x(t), p(t) and a(t), s(t) can be recalculated. The expectation of the measured signal, a(t), will equal the expectation of $x(t-\tau)$ plus the expectation of n(t), because of the linearity of the expectation operator. Because n(t) is zero-mean additive noise, its expectation will equal zero, which means that a(t) will still be given by (1), and in the frequency domain, (2) stays valid. More care is needed, however, with s(t). In the following equations s(t) is calculated as a function of p(t), x(t) and σ_n, the standard deviation of the additive noise source n(t). The notation <...> denotes the expectation operator:

$$s(t) = \langle x_m^2(t) \rangle = \langle x^2(t-\tau) + 2x(t-\tau)n(t) + n^2(t) \rangle \tag{5}$$

$$s(t) = \langle x^2(t-\tau) \rangle + 2\langle x(t-\tau) \rangle \langle n(t) \rangle + \langle n^2(t) \rangle \tag{6}$$

$$s(t) = \int_{-\infty}^{\infty} x^2(t-\tau)p(\tau)d\tau + \sigma_n^2 \quad . \tag{7}$$

When deriving (6) from (5) we used the fact that n and τ are statistically independent. As can be seen from (7) this σ_n is squared and added as a constant to (3). In the frequency domain this constant will show up as a Dirac-distribution ($\delta(\omega)$). The final set of frequency-domain equations is given by (8):

$$\begin{aligned} A(\omega) &= X(\omega)P(\omega) \\ S(\omega) &= (X*X)(\omega)P(\omega) + \sigma_n^2\delta(\omega) \quad . \end{aligned} \tag{8}$$

4. The use of a parametric model for P(ω)

According to the knowledge of the author, no algorithm is available in the literature to solve (8) for a general $X(\omega)$ and $P(\omega)$. It will be possible, however, to use a parametric model for $P(\omega)$ and to identify the parameters of this model. In literature [3] several parametric models are used to model or at least sufficiently approximate most probability density functions and associated characteristic functions appearing in practice. For the simulations and the experiments mentioned in this article the use of a normal distribution model for $p(\tau)$ appeared to be sufficient. In this section it will be explained in a more general way, however, how the parameters can be identified when a model is used for $p(\tau)$. Whatever parametric model is used, it is important to know that we can always assume that the expectation of $p(\tau)$ is equal to zero. It can theoretically be assumed that the expectation of p(t) is different from zero, but this assumption will correspond to a pure delay applied on the digitized signal. One example of a parametric model for $p(\tau)$ that is currently under investigation corresponds with a so-called Edgeworth's form of the type A series [3]. For M parameters (called κ_1 until κ_M) the model for the corresponding characteristic function $P(\omega)$ is given by (9). In this equation i refers to the

square root of -1. This model is equivalent to a truncation of the Taylor's series of log(P(ω)), the so-called cumulant-generating function and has several interesting characteristics [3]. Note that the characteristic function of a normal distribution model for $p(\tau)$ corresponds to (9) with κ_1 equal to the mean, κ_2 equal to the variation and all other κ_i's equal to zero:

$$P(\omega, \kappa_1, ..., \kappa_M) = \exp\left(\sum_{j=1}^{M} \frac{\kappa_j}{j!} (i\omega)^j \right) . \tag{9}$$

In general it will now be explained how the parameters of a parametric model for $P(\omega)$ can be identified when A and S are known. The parametric model for $P(\omega)$ will be noted as $P(\omega, \lambda_i)$, where λ_i refers to M parameters.

In order to explain the algorithm to identify the parameters λ_i, some mathematical notations will first be introduced. In practice digitized waveforms are used. The equivalent sampling time will be noted as T_s, and the number of points on the time axis used for the measurements will be called N. The fundamental angular frequency of the discrete Fourier transform (DFT) will be noted as ω_{base}, and is given by

$$\omega_{base} = \frac{2\pi}{NT_s} . \tag{10}$$

To avoid confusion a single-sided DFT is used; this means that only components will be considered with an index smaller than N/2. A subscript refers to the corresponding DFT component. A_i^M and S_i^M refer to the value of the i^{th} component of the DFT of the measured average of the digitized waveform and the average of the waveform squared. If the number of averages is increased, A_i^M and S_i^M will asymptotically tend to $A(i\omega_{base})$ and $S(i\omega_{base})$. The notation $P_i(\lambda_j)$ will refer to $P(i\omega_{base},\lambda_j)$. With these notations and conventions (8) can be written in a discrete form. The result is given by (11):

$$A_i^M = X_i P_i(\lambda_j)$$

$$S_i^M = (X_k * X_k)_i P_i(\lambda_j) + \sigma_n^2 \delta_{i0} . \tag{11}$$

An asterisk "*" denotes the single-sided DFT equivalent of a double-sided DFT circular convolution in the frequency domain, and δ_{i0} is a vector with the component with index 0 equal to 1 and all other components equal to 0. To calculate the convolution of two complex spectra, fast convolution techniques are used, performing inverse-DFT's (IDFT's), multiplications and DFT's. The fast convolution algorithm calculates the convolution as shown in (12):

$$F*G = DFT(IDFT(F)\ IDFT(G)). \tag{12}$$

In a first step X_k is eliminated by substituting X_k in the second equation of (11) by $A_k^M P_k^{-1}(\lambda_j)$. The result is written in (13):

$$S_i^M = ((A_k^M P_k^{-1}(\lambda_j))^*(A_k^M P_k^{-1}(\lambda_j)))_i P_i(\lambda_j) + \sigma_n^2 \delta_{i0} \quad . \tag{13}$$

An error vector $e_i(\lambda_j)$ is then introduced based upon (13). It is defined by (14):

$$e_i(\lambda_j) = S_i^M - ((A_k^M P_k^{-1}(\lambda_j))^*(A_k^M P_k^{-1}(\lambda_j)))_i P_i(\lambda_j) - \sigma_n^2 \delta_{i0} \quad . \tag{14}$$

To reduce the effects of noise, all components of A_i^M that have an index larger than a certain i_{MAX}, corresponding to the highest frequency component that can be distinguished from the noise, will be made equal to zero. Since a large amount of oversampling is applied, this will always be possible. Based upon this error vector an error function is introduced which is a function of the measured values A_i^M, S_i^M and of the unknown parameters λ_j. This error function $r(\lambda_j)$ is defined by (15):

$$r(\lambda_j) = \sum_{i=1}^{2i_{MAX}} |e_i(\lambda_j)|^2 \, . \tag{15}$$

Note that this error function is not a function of the unknown σ_n^2 because the index i=0 is eliminated from the summation. Also note that the largest component index in the summation is equal to $2i_{MAX}$. Considering components of $e_i(\lambda_j)$ with an index larger than $2i_{MAX}$ is theoretically possible, but will only add a constant independent of λ_j to the error function, which means that the final estimate will not be influenced. An estimate λ_j^E for the true parameters λ_j^T will be given by the value of λ_j which minimizes the function $r(\lambda_j)$. By construction, λ_j^E will be an asymptotic unbiased estimator for λ_j^T.

For the experiments and simulations mentioned in this article a Levenberg-Marquardt algorithm [4] was used to minimize $r(\lambda_j)$. The method is based on an initial guess of the parameters (e.g. parameters that correspond with the absence of jitter) and an iterative process that converges to the final solution. The algorithm is summarized in (16):

$$\lambda^{N+1} = \lambda^N + (Re(J(\lambda^N)J^+(\lambda^N) + \Lambda I))^{-1} Re(J(\lambda^N)e(\lambda^N)) \quad . \tag{16}$$

In this equation λ^N represents the N^{th} approximation of λ_j^E, J is the Jacobian of the error vector e, the superscript "+" means the transpose conjugate of a matrix, I is the identity matrix, "Re" refers to taking the real part of a complex matrix, and Λ is an algorithmic scalar parameter which systematically decreases when the algorithm is converging towards a solution. A typical stop criterion for the iteration is the convergence level reaching the computer machine precision.

Concerning the calculation of the Jacobian of the error vector, it may be useful to point out that it can easily be calculated despite the complex functional form of this error vector. The result of the calculation of the Jacobian is given in (17):

$$\frac{\partial e}{\partial \lambda_j} = -((A^M P^{-1}) * (A^M P^{-1})) \frac{\partial P}{\partial \lambda_j} + 2P\left((A^M P^{-1}) * \left(A^M P^{-2} \frac{\partial P}{\partial \lambda_j}\right)\right) \quad . \qquad (17)$$

As can be deduced from (13) an asymptotic unbiased estimate σ^2_{nEST} for σ^2_n is given by (18):

$$\sigma^2_{nEST} = S_0^M - ((A_k^M P_k^{-1}(\lambda_j)) * (A_k^M P_k^{-1}(\lambda_j)))_0 \quad . \qquad (18)$$

5. Comparison versus “median” method

Before going into the comparison between the “median” method and the extended “pdf deconvolution” method, a short overview of the “median” method [1] will be given. The idea of the “median” method is the following. Assume a strictly monotonic waveform x(t) which is being sampled at a nominal time instant T_s relative to the trigger event. Due to the timing jitter the value of our sample will not equal $x(T_s)$ but will equal $x(T_s-\tau)$, with τ being a stochastic variable. In a set of many samples taken at the nominal time T_s, about half of the samples will be taken at time instants earlier than T_s and the other half at instants later than T_s. Because of the strict monotonicity of x(t), this also means that the value of about half of the samples will be lower than $x(T_s)$ and the other half higher. To have a good estimation of $x(T_s)$ it is sufficient to calculate the median of all sample values. It is easy to prove that this estimator is asymptotically unbiased for monotonic waveforms when no additive noise is present. Unfortunately most waveforms that are measured are not monotonic. When this is the case all maxima and minima will be clipped [1], and no matter how many measurements are performed, this distortion can never be compensated. The inevitable presence of additive noise, presumed to be white with zero mean, will also cause a bias. This fact, not mentioned in [1], can be explained by the fact that the relation between the pdf of sampled values at a certain T_s when additive noise is present equals the ideal additive-noise-free pdf convolved with the pdf of the additive noise. Since the median of a distribution is by no means invariant with respect to convolutions if the distribution is nonsymmetric (even when the distribution to convolve with is a zero mean normal distribution), the presence of the additive noise will cause a bias in all points where the pdf of the sampled values is nonsymmetric.

In order to compare the performance of the “median method” with the newly developed method, software was written simulating the jitter process. The idea was to define an analytically described pulse. For convenience the impulse response of a third-order, Butterworth, low-pass filter was chosen. From this analytically defined waveform sampled versions could easily be calculated. This pulse corresponds to the theoretical x(t) in the previous derivation. Then several time-jittered versions were constructed by evaluating x(t), not at instants nT_s, but at instants $nT_s-\tau$, with τ being a random number, different for each different version as well as for each sample. By applying the desired “numerical recipe” [5] many different probability density functions can be constructed out of the RANDOM numbers created by the computer (which usually have a uniform distribution). The average of all jittered versions was then calculated as well as the average of all jittered versions squared. These two functions are the estimates for a(t) and s(t) and are transformed into the frequency domain by an FFT, resulting in $A(\omega)$ and $S(\omega)$. The algorithm of section 4 was then applied with a normal distribution model for $p(\tau)$. This resulted in an estimate for $P(\omega)$. Using the method as described by Gans [2] to deconvolve this $P(\omega)$ from $A(\omega)$ resulted in an estimate for $X(\omega)$. The “median method” estimator

was also applied to the jittered waveforms, so finally the quality of both methods could be compared. For the simulation the following parameters were chosen:

x(t): impulse response of a third-order, low-pass, Butterworth filter with ω_{cut}=1 rad/s or,

$$x(t)=\begin{cases} e^{-t}+\left(\frac{1}{\sqrt{3}}\sin\left(\frac{\sqrt{3}}{2}t\right)-\cos\left(\frac{\sqrt{3}}{2}t\right)\right)e^{-\frac{t}{2}} & \text{for } t >= 0 \\ 0 & \text{for } t < 0 \end{cases} \qquad (19)$$

Applied jitter noise: Gaussian with σ_{jitter} = .75 seconds

Applied additive noise: Gaussian with σ_n= 0.03 volts

T_s: 0.3 seconds (sampling time)

Number of samples: 256

Start time: -10 seconds (stop time = 66.5 s)

Nyquist frequency = 5/3 Hz

Number of simulated waveforms used for averaging : 3000
Number of simulated waveforms used for median estimate: 3000.

The results of the simulation are shown in Fig. 1 through Fig. 4. A discussion on these results is noted in what follows.

Figure 1 and Fig. 2 show the results of both methods in the time domain. The “median” method underestimates the maximum voltage of the true waveform by about 12%, while the error for this maximum voltage is only about 0.25% with the extended “pdf deconvolution” method. The large error for the “median” method is due to the previously mentioned clipping effect [1]. As can be seen from Fig. 1 and Fig. 2 the “pdf deconvolution” method can accurately estimate the maximum voltage, but it introduces a ringing effect which is not present with the “median” method. This ringing is typical for the deconvolution process, and can also be noted in the results of Gans [2]. The bias introduced by the “median” method due to the presence of additive noise can be seen when looking at the voltage values for time instants close to 0 seconds. A bias is present, although the waveform is perfectly monotonic at this time instant. This is in agreement with the theory as explained in the beginning of this section.

Figure 3 and Fig. 4 show the results of both methods in the frequency domain. The result of the “median” method is significantly biased at all frequencies. This can easily be explained by the clipping effect. The result of the “pdf deconvolution” method is very accurate for frequencies smaller than 0.2 Hz, but the results for frequencies higher than 0.3 Hz are very inaccurate. This 0.3 Hz corresponds to the frequency where the spectral components of A(ω) have amplitude values which become comparable to the noise floor. Such a frequency will always be present for the “pdf deconvolution” method. It is a limit for the method, which causes the estimates of the spectral components of the true signal to be accurate only for frequency components smaller than a certain limit frequency. This fact causes the time-domain ringing effect mentioned above. Note that the limit frequency will increase when more averaging is applied because this will result in a lower value for the noise floor. Such a limit frequency does not exist for the “median” method. This method will be able to estimate the values of spectral com-

ponents with frequencies that are considerably higher than the “pdf deconvolution” method frequency limit. Note, however, that the estimates will be biased.

To conclude it can be said that the decision of which method to choose depends upon the application. When ringing can be allowed or an accurate estimate is needed of signal spectra, the extended “pdf deconvolution” method gives very good results. If the waveform is monotonic and there is not too much additive noise present, the “median” method is preferable.

6. Asymptotic bias of the classical way to estimate the jitter pdf

In this paragraph the problems mentioned in the introduction, concerning the method to determine the jitter pdf as mentioned in [2], will be illustrated.

Suppose we are sampling the waveform described by (19), with the same jitter pdf as in the previous section, but with no additive noise present. In this case the method as described in [2] would use the measurement of the slope of the averaged waveform at a certain time instant, which will be called $\tan\theta$, together with the standard deviation of the vertical noise at this instant, called σ_M, to estimate the jitter standard deviation σ_{jitter}. The relation between the two measured quantities and the estimate of the jitter standard deviation, denoted by $\bar{\sigma}_{jitter}$, is then given by (19):

$$\bar{\sigma}_{jitter} = \frac{\sigma_M}{\tan\theta}. \tag{19}$$

It is easy to show [2] that this method gives an asymptotic unbiased estimate for σ_{jitter} if applied to an ideal ramp. If applied to pulselike signals, however, with a jitter standard deviation which is significant relative to the pulse transition duration, an asymptotic bias will result on the estimation of σ_{jitter}. This will cause an error on the estimation of the spectrum of the undistorted signal. We will illustrate this on the waveform as described by (19).

We choose the time instant to measure σ_M and $\tan\theta$ equal to 0.8 seconds. This instant is chosen such that the value of the averaged waveform is about half the maximum value achieved. At this instant the pulselike signal can best be approximated by a ramp. Next the conditions of the previous section are used and 3000 jittered waveforms are simulated. The averaged waveform is calculated for time instants equal to 0.5, 0.8 and 1.1 seconds. The result is given in the following table.

time instant (seconds)	averaged value (volts)
0.5	0.1345
0.8	0.1821
1.1	0.2403

From these three values, the value of $\tan\theta$ is estimated to be equal to 0.1763 volts/second. This value is calculated by using linear regression. Next the standard deviation σ_M is calculated for a time instant equal to 0.8 seconds. The result is 0.1450 volts. Using (19) this results in a value for $\bar{\sigma}_{jitter}$ equal to 0.8224 seconds. The exact value of σ_{jitter} is equal to 0.75 seconds. We can conclude that there will be an asymptotic bias of about 10% on the estimate of σ_{jitter}, due to

the fact that the waveform is not an ideal ramp. When this biased value of σ_{jitter} is used in the deconvolution algorithm the error in the estimation of the spectral component with a frequency of 0.2 Hz would be about 0.8 dB. This asymptotic bias is not present when the method is used as described in section 4. It is important to note, however, that the bias mentioned in this section becomes negligibly small when the waveform can be approximated very well by a ramp over an interval large compared to σ_{jitter}. In such a case both methods have the same accuracy, but the method described by Gans [2] is much simpler to implement.

7. Experimental results

Finally an experimental setup was made to check the new method in practice. To accomplish this, a pulse generated by a step recovery diode (SRD) was measured by an HP-54120 sampling oscilloscope, and the extended "pdf deconvolution" method was applied. To control the amount of jitter a controllable attenuator was introduced in the trigger signal path. By attenuating the trigger signal the amount of jitter could artificially be enlarged. Then it became possible to compare the reconstructed waveforms with less and the ones with more jitter. This way it can be shown that the reconstructed waveforms are insensitive to jitter and that the method works well. The results of the experiment are shown in Fig. 5 through Fig. 7. The SRD was excited by a 97.65625 MHz sine wave; the oscilloscope took 1024 samples with a sampling time equal to 10 picoseconds. For calculating the point-by-point average of the waveforms and the waveforms squared, 1000, 2000 and 4000 averages were used corresponding to 0 dB, 10 dB and 15 dB of attenuation in the trigger path, respectively.

Figure 5 shows the spectra of the three averaged waveforms, corresponding to an attenuation of 0 dB, 10 dB and 15 dB respectively. The low-pass filtering effect of the jitter can clearly be distinguished. At 7 GHz, for example, the third spectrum (15 dB of attenuation in trigger path) has an attenuation of 30 dB relative to the first spectrum (0 dB of attenuation in trigger path). Figure 6 shows the same spectra when the extended "pdf deconvolution" method has been applied. The parametric model that was used for the pdf corresponds to a normal distribution. Now the three spectra are practically coincidental. The fact that the third spectrum no longer corresponds to the other two above 7 GHz is due to the fact that at 7 GHz the spectrum of the averaged third waveform goes down into the noise floor. This means that the compensating filter will be amplifying noise for this spectrum once above 7 GHz. Figure 7 shows the differences between the reconstructed spectra with 10 dB and 15 dB of attenuation in the trigger path relative to the reconstructed spectrum with 0 dB in the trigger path. This shows that the three spectra correspond very well for those frequencies where the averaged waveform spectrum does not reach the noise floor (correspondence within about 200 mdB). Two parasitic effects can be distinguished. First an offset of about 200 mdB is noticed in Fig. 7. This can be explained by the fact that the different experiments took place over a very long period (a whole night) and that there might have been a small gain drift of the oscilloscope during the experiment. A second effect is the difference being substantially larger for the first 5 frequency components. This is probably caused by a leakage effect of the periodic excitation component of the SRD which is dominantly present in the measurement (cf. the peak near DC in Fig. 5 and Fig. 6). Although the frequency of this component was chosen carefully to avoid leakage, an inevitable small error in the oscilloscope's timebase accuracy will still cause a small amount of leakage of this component, having a power about 11 dB higher than the surrounding components. Because the phase of this leaky component is different relative to the sampling window whenever another attenuation level is used in the trigger path, its effect will be different from experiment to experiment and this will show up as it does in Fig. 7.

The estimated values for the jitter standard deviation for the three cases are 6.4 ps, 15.8 ps and 57.6 ps respectively.

8. Conclusion

A new method has been described for the determination of the characteristic function of the jitter pdf. This method can be used to extend the “pdf deconvolution” method as described by Gans [2] to cases where the waveform can not be approximated by a ramp at any time instant, which is the case for pulselike signals when the standard deviation of the jitter is no longer small compared to the pulse transition duration. The method uses the average and the average of the square of a large set of recorded waveforms. It has been shown that the method is especially useful when a correct reconstruction of the spectrum is required.

9. Acknowledgment

The author would like to thank Yves Rolain for helpful discussions, Rik Pintelon and Johan Schoukens for critically reading the manuscript, Prof. Alain Barel for providing the instruments needed for the measurements and the NFWO (Belgian National Fund for Scientific Research) for the support under reference 2.0114.90.

References

[1] T. Michael Souders, Donald R. Flach, Charles Hagwood and Grace L. Yang,“The effects of timing jitter in sampling systems,” IEEE Trans. Instrum. Meas., vol. IM-39, Feb.1991.

[2] W.L. Gans,”The measurement and deconvolution of time jitter in equivalent-time wave form samplers,” IEEE Trans. Instrum. Meas., vol. IM-32, Mar. 1983.

[3] M. Kendall, A. Stuart and J. K. Ord,”Advanced Theory of Statistics,” Charles Griffin & Company Limited, vol. 1, 1987.

[4] Marquardt D. W.,”An algorithm for least-squares estimation of nonlinear parameters,” SIAM J., 1963.

[5] William H. Press, Brian P. Flannery, Saul A. Teukolsky, William T. Vetterling, “Numerical Recipes,” Cambridge University Press, 1987.

Short biographic sketch

Jan Verspecht was born in Merchtem, Belgium, on December 12th, 1967. He received the degree of engineer in 1990 from the University of Brussels (VUB).

As a member of the Hewlett-Packard Network Measurement and Description Group, he is currently working towards the Ph.D. degree at the University of Brussels (VUB). His subject is advanced calibration methods for measuring nonlinear microwave devices.

Figure captions

Fig. 1

Analytical versus reconstructed pulses
Y-scale in volts
X-scale in seconds
solid line: analytical
dot-dashed line: extended “pdf deconvolution” method
dashed line: “median” method

Fig. 2

Difference between analytical and reconstructed pulses
Y-scale in volts
X-scale in seconds
dot-dashed line: extended “pdf deconvolution” method - analytical
dashed line: “median” method - analytical

Fig. 3

Spectra of analytical and reconstructed waveforms
Y-scale in dBV
X-scale in Hz
solid line: analytical
dot-dashed line: extended “pdf deconvolution” method
dashed line: “median” method

Fig. 4

Spectral difference between reconstructed waveform and analytical waveform
Y-scale in dB
X-scale in Hz
dot-dashed line: extended “pdf deconvolution” method - analytical
dashed line: “median” method - analytical

Fig. 5

Measured spectra of averaged SRD-pulse with different attenuation in trigger path
Y-scale in dBm
X-scale in GHz
solid: 0 dB of att. in trigger path
dashed: 10 dB of att. in trigger path
dot-dashed: 15 dB of att. in trigger path

Fig. 6

Spectra of reconstructed spectra with different attenuation in trigger path
Y-scale in dBm
X-scale in GHz
solid: 0 dB of att.
dashed: 10 dB of att.
dot-dashed: 15 dB of att.

Fig. 7

Spectral difference between reconstructed waveforms with different attenuation in trigger path
Y-scale in dB
X-scale in GHz
thick line: “10 dB of att.” - “0 dB of att.”
thin line: “15 dB of att.” - “0 dB of att.”

Fig.1

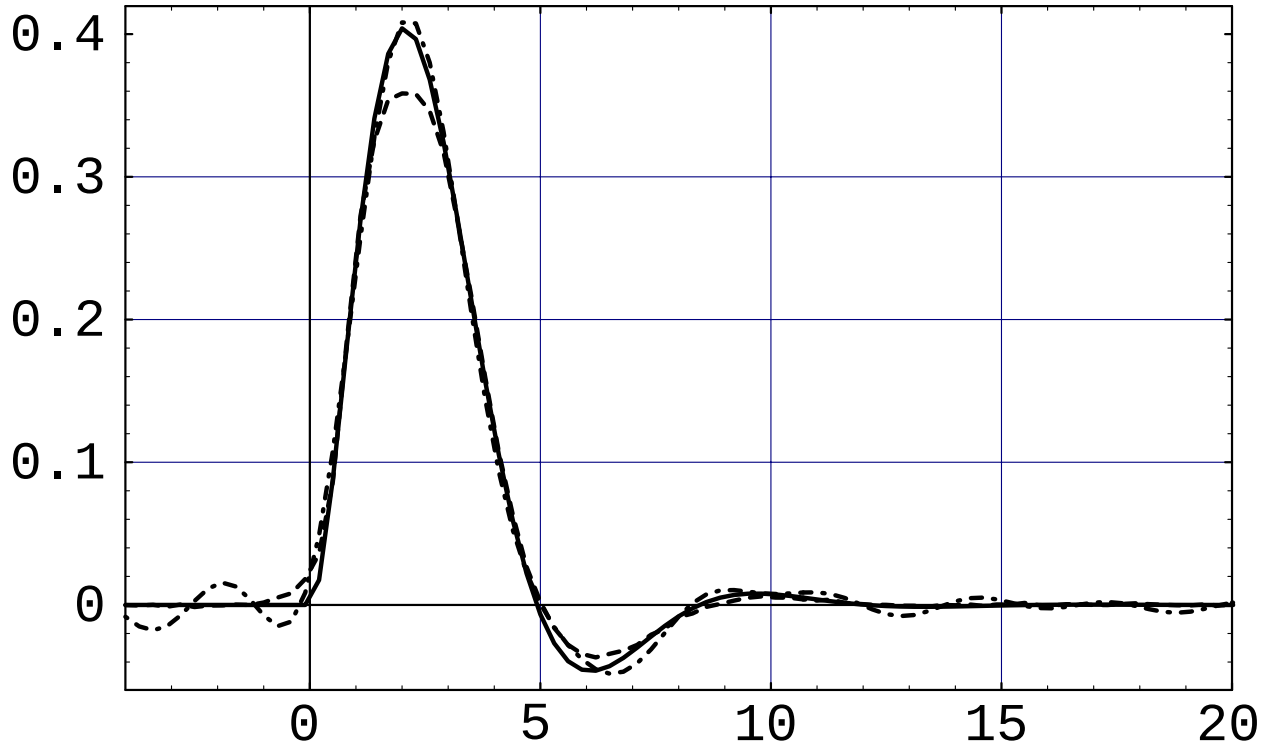

Fig.2

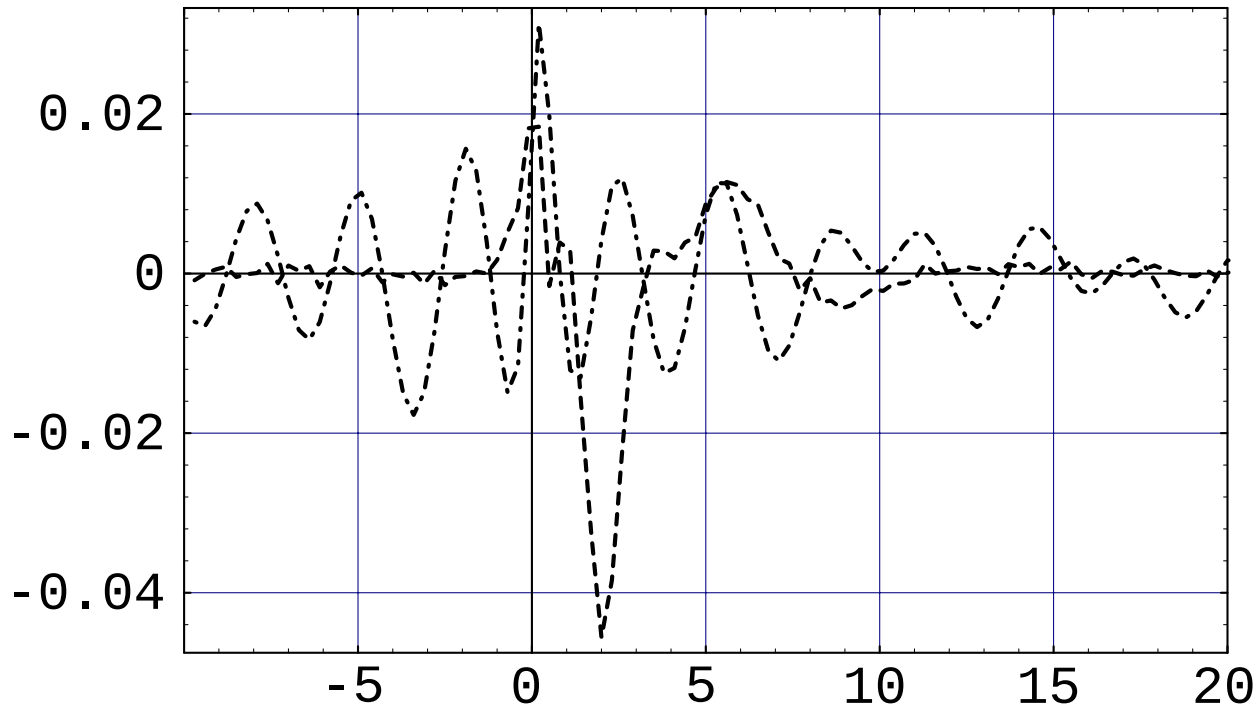

Fig.3

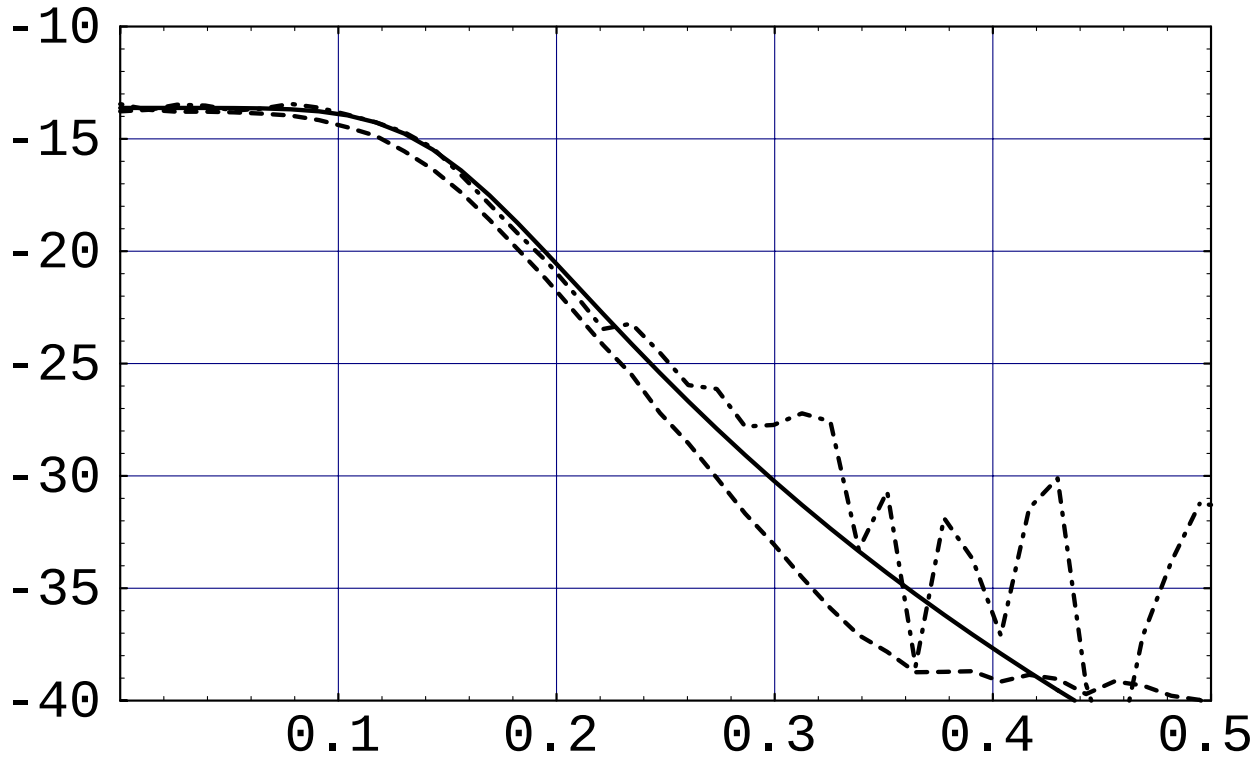

Fig.4

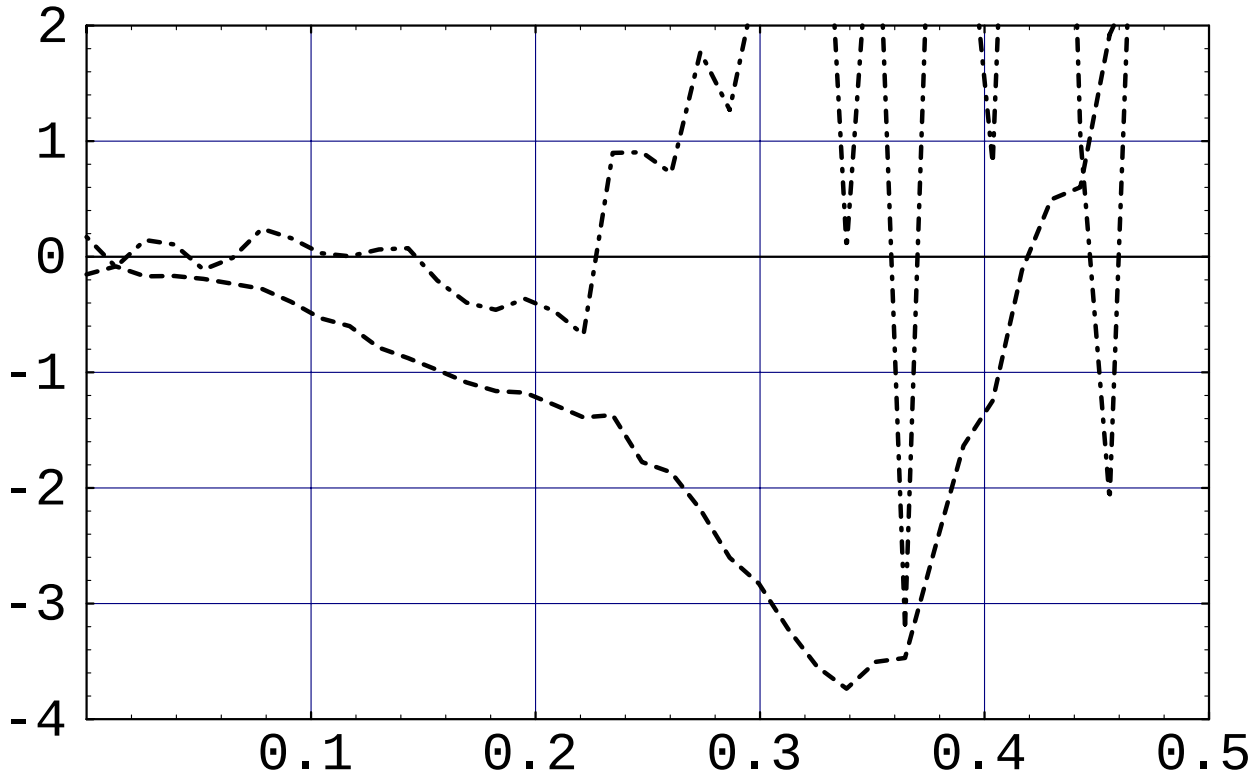

Fig.5

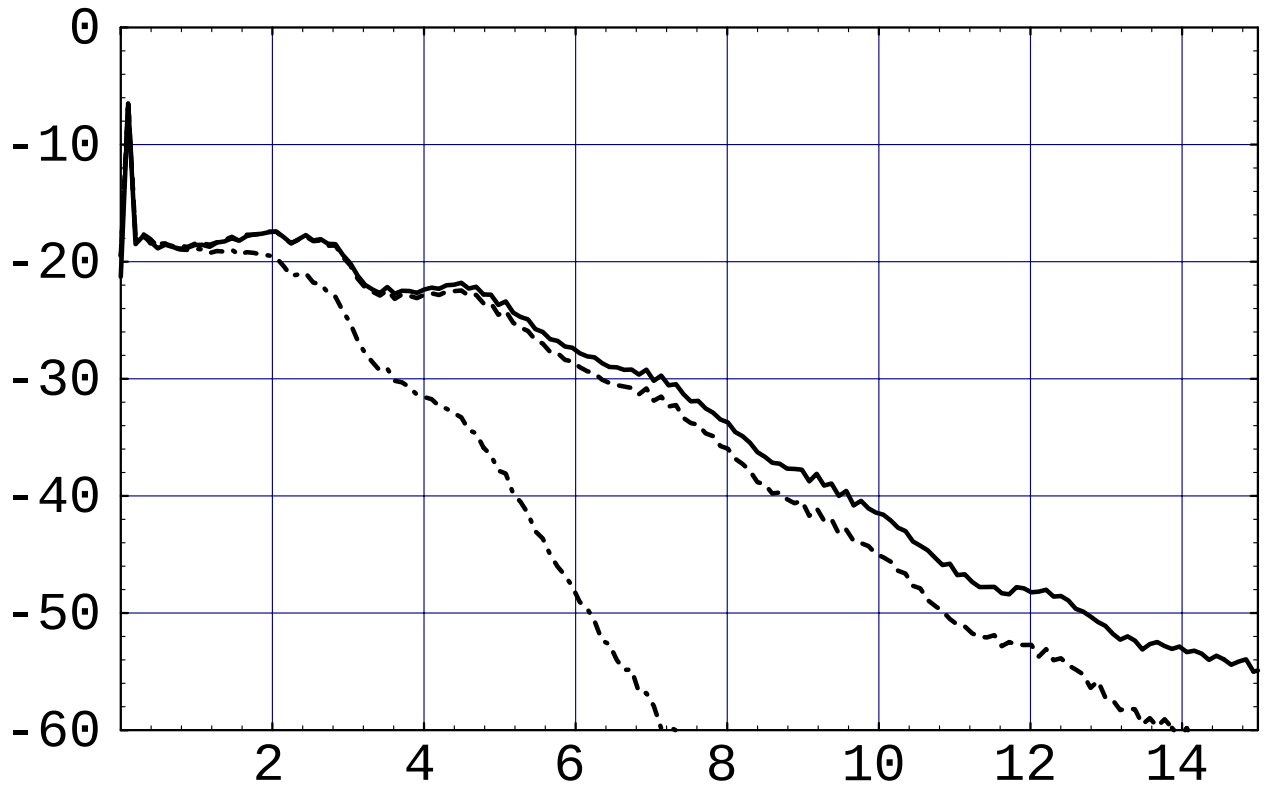

Fig.6

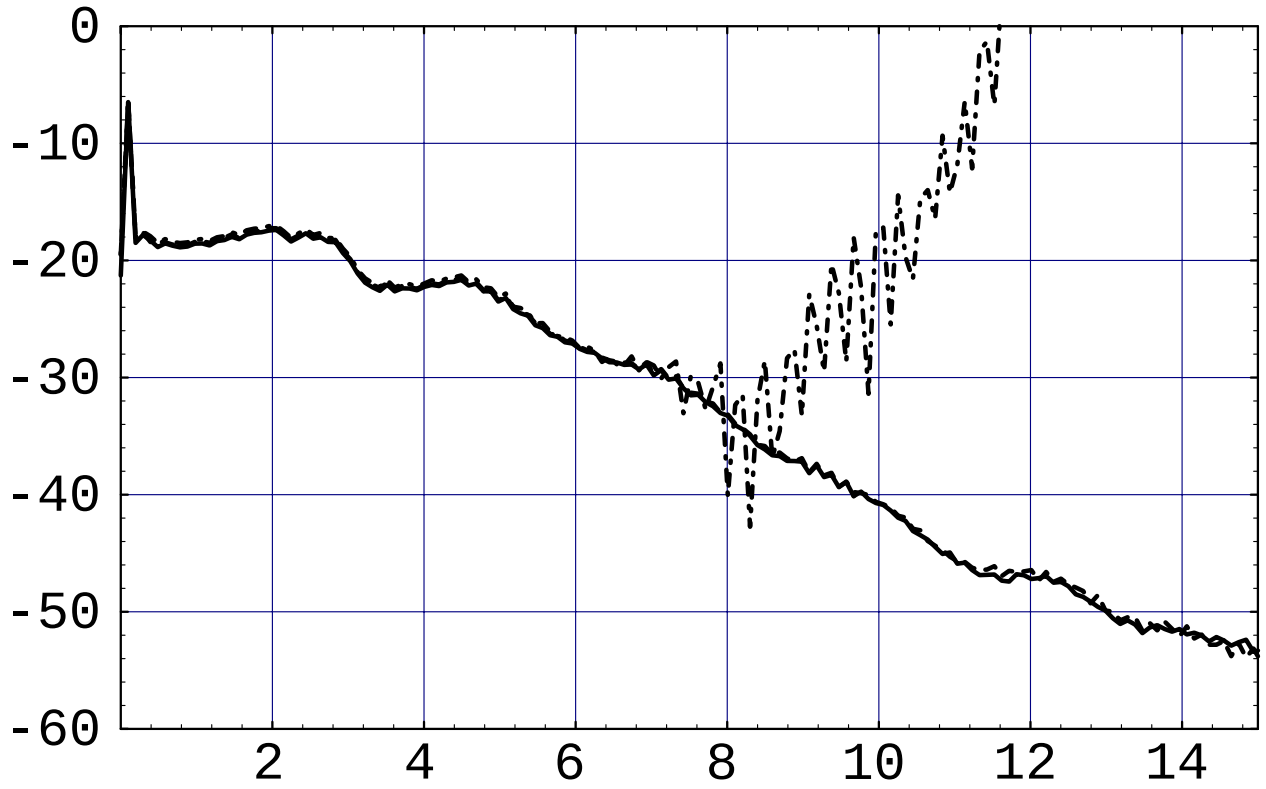

Fig.7